Journal of Archaeological Science 52 (2014) 458–467

Contents lists available at ScienceDirect

Journal of Archaeological Science

journal homepage: http://www.elsevier.com/locate/jas

Feasibility studies of Sn isotope composition for provenancing ancient bronzes

E. Yamazaki [a, b], S. Nakai [a, *], Y. Sahoo [a], T. Yokoyama [b], H. Mifune [c], T. Saito [d], J. Chen [e], N. Takagi [a], N. Hokanishi [a], A. Yasuda [a]

[a] Earthquake Research Institute, The University of Tokyo, 1-1-1 Yayoi, Bunkyo-ku, Tokyo, 113-0032, Japan
[b] Department of Earth and Planetary Sciences, Tokyo Institute of Technology, 2-12-1 Ookayama, Meguro-ku, Tokyo, 152-8851, Japan
[c] Faculty of Art and Design, Toyama University, 180 Futagami, Takaoka, Toyama, 933-8588, Japan
[d] National Museum of Japanese History, 117 Jonai-cho, Sakura City, Chiba, 285-8502, Japan
[e] School of Archaeology and Museology, Peking University, No. 5 Yiheyuan Road Haidian District, Beijing, 100971, 100871, P.R. China

ARTICLE INFO

Article history:
Received 7 December 2013
Received in revised form
15 September 2014
Accepted 17 September 2014
Available online 28 September 2014

Keywords:
Sn isotope composition
Bronze
Cassiterite
Casting experiment
ICP–MS
China

ABSTRACT

This study examined isotope fractionation during bronze casting and assessed variation in Sn isotope composition of Chinese bronze products to ascertain whether a Sn isotope tracer is applicable to provenance studies of bronze products or not. A casting experiment revealed that the Sn isotope composition of a bronze block surface becomes slightly heavier, 0.22‰ in $\delta^{124}Sn/^{120}Sn$ scale, ($\delta^{124}Sn/^{120}Sn = [(^{124}Sn/^{120}Sn_{sample})/(^{124}Sn/^{120}Sn_{standard}) - 1] \times 10^3$), than original Sn beads because of selective evaporation of light isotopes. The Sn isotope compositions of six bronze product samples excavated in China were analyzed. The variation of $\delta^{124}Sn/^{120}Sn$ in the six samples was as great as 0.4‰. Six bronze samples showed small but detectable isotope variation that surpassed isotope shift during casting. Results suggested that the application of Sn isotope ratio to provenance studies of bronze products was of limited use because of the small variation. However, it was also shown that the Sn isotope ratio can be applied for provenancing a bronze sample with a distinct isotope composition.

1. Introduction

Bronze consists primary of copper. Tin (Sn) was mixed as an additive to produce a hard and tough metal with copper, the main component of bronze. Bronze came into use in the mid-fifth millennium BC. Radivojević et al. (2013) recently reported tin bronze artifacts dated to the mid-fifth millennium BC in the Balkans, although the influence of the culture to other areas, remains to be investigated. In Mesopotamia, bronze production started in the early third millennium BC and bronze subsequently spread to Europe and Asia. In China, the Bronze Age started in the early second millennium BC. A highly sophisticated bronze technology was developed during the Shang Dynasty by the late second millennium BC (Rapp, 2009). The provenance of bronze has been investigated using Pb isotope compositions together with other metal products (Stos-Gale and Gale, 2009). However, because Pb in bronze derives mostly from the Cu source or Pb source itself, the Pb isotope composition of bronze reveals little about the Sn source. Scarce knowledge of Sn deposits used in ancient times, especially in eastern Asia, also hinders Sn provenance studies.

Tin has 10 stable isotopes with isotope masses of 112–124. This number of stable isotopes is the highest among all elements in the periodic table. Although meteorites have been analyzed since the 1960s (De Laeter and Jeffery, 1965; Loss et al., 1990), no isotope anomaly has been confirmed for them because of the limited precision of isotope analyses. Terrestrial samples have also been analyzed by several groups (Clayton et al., 2002; De Laeter and Jeffery, 1965, 1967; Haustein et al., 2010; McNaughton and Loss, 1990; McNaughton and Rosman, 1991; Rosman and McNaughton, 1987; Yamazaki et al., 2013). Among these studies, Haustein et al. (2010) reported the largest Sn isotope variation (0.55‰ per unit mass difference) in a terrestrial Sn mineral, cassiterite, from the Erzgebirge region (Germany) and Cornwall (Great Britain). Cassiterite has been widely used as a raw material for Sn metal and bronze alloys since ancient times. Therefore, Haustein et al. (2010) reported the possible application of Sn isotope analysis to studies of bronze provenance. In contrast, Yamazaki et al. (2013) reported rather limited variation of Sn isotope composition (0.19‰ per unit

* Corresponding author.
E-mail address: snakai@eri.u-tokyo.ac.jp (S. Nakai).

http://dx.doi.org/10.1016/j.jas.2014.09.014
0305-4403/

mass difference) in Asian cassiterites from Japan, China, Thailand, and Malaysia, suggesting that highly precise Sn isotope analysis is necessary to perform provenance studies of bronze in Asia.

Apart from application to provenance studies, the application of Sn to detect the use of recycled bronze was proposed by Budd et al. (1995). Budd et al. (1995) reported a potential risk associated with provenancing bronze using a Pb isotope tracer by evaporation during extraction and manufacturing processes. Budd et al. (1995) pointed out the possibility that bronze was re-melted many times. For that reason, Pb isotopes might have been changed by fractionation induced by evaporation. Nevertheless, detecting isotope variation in recycled bronzes using a Pb isotope tracer is not easy because the natural variation of the Pb isotope composition in Pb ores is also large. In addition, Stos-Gale and Gale (2009) disproved large-scale lead isotope fractionation during ancient metallurgical processes by comparing Athenian silver coins and Lavrion ore deposit in Attica. Budd et al. (1995) suggested that Sn isotope compositions of bronze can be fractionated during melting because of its volatility, and suggested that Sn isotope compositions are useful as tracers to detect bronze recycling because the natural variation of the Sn isotope composition is limited. Gale (1997), however, reported that the variation of $^{122}Sn/^{116}Sn$ in ancient bronzes was less than 1‰ and concluded that the influence of recycling was not so strong. Therefore, variations in Sn isotope composition in bronze are an important research target for archaeology (Haustein et al., 2010; Nickel et al., 2012).

Although early Sn isotope analyses were performed using thermal ionization mass spectrometry (TIMS; De Laeter and Jeffery, 1965, 1967; Devillers et al., 1983; Gale, 1997; Loss et al., 1990; McNaughton and Loss, 1990; McNaughton and Rosman, 1991; Rosman and McNaughton, 1987; Rosman et al., 1984), the high ionization potential of Sn (7.3 eV) hindered Sn ionization by TIMS, leading to moderate precision of isotope analyses. Since the development of multi-collector inductively coupled plasma mass spectrometry (MC–ICP–MS) with high ionization efficiency, Sn isotope analyses have been performed mainly using MC–ICP–MS (Balliana et al., 2013; Clayton et al., 2002; Haustein et al., 2010; Lee and Halliday, 1995; Moynier et al., 2009; Nickel et al., 2012; Osawa et al., 2009; Yamazaki et al., 2013). The present study analyzed Sn isotope compositions in six Chinese bronze samples using MC–ICP–MS and compared the results with isotope variations in cassiterites described in previous reports (Yamazaki et al., 2013). We also examined a casting experiment to assess the possibility of Sn isotope fractionation via evaporation. Combining results of the two investigations, we then assess the feasibility of applying a Sn isotope tracer to studies of bronze provenance.

2. Sample description

Six bronze samples excavated from China were analyzed in this study (Table 1). Chemical compositions of the samples determined using SEM-EDS analysis are presented in Table 1. Fig. 1 portrays the sampling sites together with the localities of cassiterite ore deposits with Sn isotope compositions reported by Yamazaki et al. (2013). Bronze samples 1807, 1813, 1827-3, and 1829 were excavated from Panlongcheng site in Huangpi, Hubei Province. The site, an important city of the Early Shang Dynasty, is about 40 km from Wuhan, north of the Yangtze River. The styles and patterns of bronze excavated from Panlongcheng resemble those of bronze from the Erligang period excavated in the Yellow River Basin. The Panlongcheng site is regarded as a transfer station to control strategic resources in southern China, such as copper for the Shang Dynasty. Samples 1807 (knife) and 1813 (arrowhead) were unearthed from the Wangjiazun site in the Panlongcheng. They were heavily corroded. Only pieces of fragments remained. The samples used for analyses were taken from these fragments. Both samples were cast in lead–tin bronze. A sample 1827 (Jue, container) was collected from the No. 1 tomb of Lijiazui site in Panlongcheng. Of the four pieces of Jue buried in the tomb, three of them (PLZM1: 15, PLZM1: 16, and PLZM1: 17) were well preserved. The sample analyzed in this study, PLZM1: 18, was heavily corroded and broken into the object's rim, abdomen, foot, and other parts (Hubei Provincial Institute of Cultural Relics and Archaeology (2001)). The 1827-3 was sampled from the abdomen part. This sample was also cast in lead–tin bronze.

The Liulihe site is 43 km southwest of Beijing city. More than 200 tombs constructed by the Yan state have been excavated. The most important tomb is the largest tomb, M1193, with four tunnels that can be dated to 1015BC–985BC. The owner of Tomb M1193 might be the first marquis of Yan state and the first son of Shaogong (Liulihe Archaeology Team, 1990). Two bronze samples (1950 and 1953) were collected from this tomb. The sample 1950 (mask) is about 21 cm high and 22.3 cm wide. It has a narrow brow, round eyes, a wide nose, and a big mouth. Sample 1953 (round ornament), a hemispherical drum shape of about 10 cm diameter, could have been decorated with a painted shield or leather armor.

Casting experiments were conducted at Toyama University. High-purity (99.99%) Cu and Sn beads were purchased from Kojundo (High Purity) Chemical Lab. Co. Ltd., Saitama, Japan. The Sn beads were of 4–6 mm diameter. Cu and Sn were mixed with a ratio of 85:15. A 40 mm × 55 mm × 40 mm (depth) bronze block was produced (Fig. 2a) in a mold prepared using clay as follows. Copper and Sn beads were melted in a graphite pod comprising 35–45% of C and 30–50% SiC (Morex CA-5; Tokyo Morex Crucible Co., Ltd.) at 1100–1200 °C for about 20 min. Melted metal was poured into the mold (Fig. 2b). About 93% of the starting material was recovered in the bronze block. The block surface temperature dropped below 800 °C within a few minutes. A 5-mm-thick slice was cut from the center of the block (Fig. 2a). A 5-mm-thick reed-shaped column was cut from the center of the slice (Fig. 2c). The top, center, and bottom of the column were used for Sn isotope analyses after parts of a few millimeters from the surface and bottom were removed (Fig. 2c). Each block was approximately 3 mm × 5 mm × 5 mm.

Table 1
Samples analyzed in this study.

Sample number	Artifacts	Sampling position	Site	Age	Dynasty	Cu[a] (wt.%)	Sn[a] (wt.%)	Pb[a] (wt.%)	Fe[a] (wt.%)
1807	Knife		Panlongcheng, Hubei Province	B.C. 1400	Shang	83.5	11.3	5.2	0.08
1813	Arrowhead		Panlongcheng, Hubei Province	B.C. 1400	Shang	83.0	9.5	7.5	<0.05
1827-3	Jue (container)		Panlongcheng, Hubei Province	B.C. 1400	Shang	73.9	8.7	17.2	0.14
1829	Decoration ware		Panlongcheng, Hubei Province	B.C. 1400	Shang	75.4	11.9	12.7	0.10
1950	Mask	Edge	Liulihe, Fangshan District, Beijing	B.C. 1000–900	Western Zhou	77.6	9.8	10.1	0.58
1953	Round ornament	Edge	Liulihe, Fangshan District, Beijing	B.C. 1000–900	Western Zhou	81.8	14.2	4.0	<0.05

[a] Chemical compositions of the bronzes were analyzed at the National Museum of Japanese History (see Section 3).

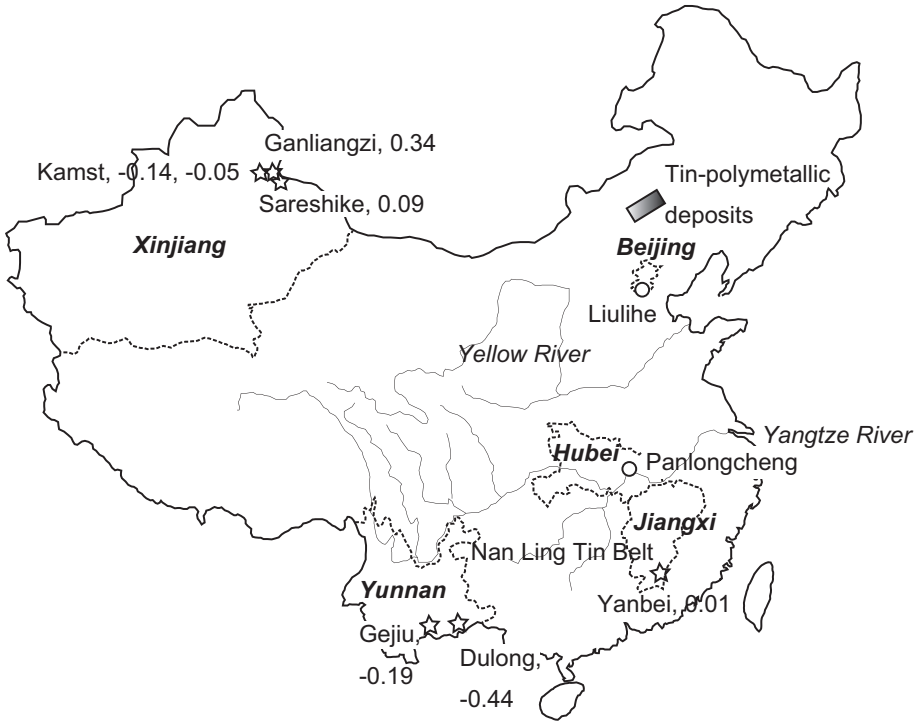

Fig. 1. Location map of the excavated sites of bronze products analyzed in this study (shown as black circles) and the sites of cassiterite deposits reported in Yamazaki et al. (2013) (shown as stars). Numerical value close to a name of deposit is $\delta^{124}Sn/^{120}Sn$ of cassiterite from the deposit (Yamazaki et al., 2013). Locations of tin-polymetallic deposits in the southern part of Da Hinggan Mountains (Wang et al., 2005) and NanLing Tin Belt (Penhallurick, 1986) are also shown.

3. Analytical methods

We fundamentally followed the Sn isotope analytical method presented by Yamazaki et al. (2013). The procedure is described briefly as follows. Reagents, TRU resin and polypropylene column used for this study were described by Yamazaki et al. (2013). PFA vials (Savillex Corp.) were used to decompose bronze samples. Bronze sample solutions were stored in LDPE bottles (Nalgene).

A commercial Sn solution (CLSN2-2Y, Lot#CL5-45SN; SPEX CertiPrep Inc.) was used as the isotope and concentration standard. In this report, all Sn isotope data measured using MC–ICP–MS are presented in δ notation against the SPEX standard solution. The Sn isotope composition of this standard solution was compared with that of NIST SRM 3161a. The $\delta^{124}Sn/^{120}Sn$ of this standard was reported as 0.30 ± 0.06‰ in $\delta^{124}Sn/^{120}Sn$ scale (Yamazaki et al., 2013). In addition, an Sb (antimony) standard solution (Cat#PLSB7-2Y, Lot#13-134SB; SPEX CertiPrep Inc.) was used to correct for mass biases in Sn isotope analysis using MC–ICP–MS (Clayton et al., 2002).

Some samples of archaeological and cast bronze could not be dissolved in pure HCl. Samples of bronze and Sn beads were dissolved in mixtures of 1.5 mL of 10 M HCl (#18078-1B; Kanto Chemical Co. Inc.) and 0.25 mL of 13.4 M HNO_3 (#28163-1B; Kanto Chemical Co. Inc.). No residue was observed. Dissolution experiments were conducted using two pairs of split Sn beads. One part was dissolved by the mixture acid described above and another by pure HCl. The values of $\delta^{124}Sn/^{120}Sn$ of a part dissolved in the mixture acid were 0.06 ± 0.10 and 0.01 ± 0.08‰ relative to a part dissolved in pure HCl. Consequently, the usage of HNO_3 did not cause isotope fractionation. Bronze solution was aliquotted so that the fraction contained around 2 μg of Sn. After the aliquot was evaporated, it was dissolved in 2 mL of 0.5 M HCl for purification. The Sn beads were diluted with 0.4 M HNO_3 solution to around 100 ppb and were analyzed without purification. Sn was purified from sample solutions of bronze with a TRU resin (TRU resin, particle size, 100–150 μm, #TRU-B50-A; Eichrom Technologies, Inc.) as follows.

The TRU resin was put into a Teflon vial with 0.4 M HNO_3 for precleaning at 50 °C for 4–5 h. After the resin particles that floated were removed using a pipette, 0.4 M HNO_3 was added to the vial. This procedure was repeated three times. The thus pre-cleaned TRU resin was stored in 0.4 M HNO_3. Then 1 mL of TRU resin was charged in a polypropylene column. Detailed procedures used to separate Sn are presented in Table 2. We collected Sn in 16 mL of 0.4 M HNO_3 solution, immediately followed by the addition of 0.285 mL of 0.1 M HF to the Sn fraction to prevent Sn precipitation (Yi et al., 1995). A Sn blank for the purification process was around 10 ng. The recovery and isotope fractionation of Sn during the purification procedure were examined using a mixed standard solution including 50 elements (Yamazaki et al., 2013). Recoveries of Sn were better than 95%. The isotope fractionation of Sn during the separation procedure was measured as −0.66 ± 0.09‰ in $\delta^{124}Sn/^{120}Sn$ scale. We use this factor when discussing the isotope compositions of Chinese archaeological bronzes.

For samples obtained from a casting experiment, we modified the procedure described above. After we purified Sn with TRU resin, the solution containing Sn was nearly evaporated to dryness and then dissolved in 0.4 M HNO_3. By this modification, isotope fractionation during purification was reduced to −0.10 ± 0.08‰, probably because organic matter was decomposed. This fractionation factor was obtained using similar experiments as those conducted by Yamazaki et al. (2013) using a bronze simulating solution. We use this factor when discussing isotope compositions of samples derived from the casting experiment.

Tin isotope ratios were measured using an MC–ICP–MS (IsoProbe; Micromass Ltd.) installed at the Earthquake Research Institute of The University of Tokyo. Sample solutions were introduced through a desolvation system: ARIDUS (CETAC Co.). We monitored

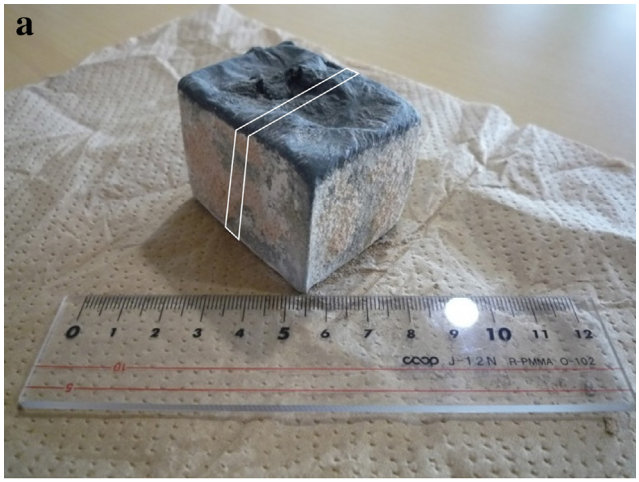

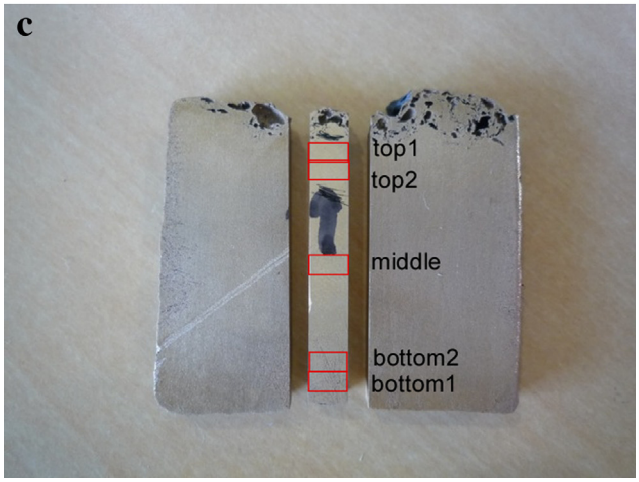

Fig. 2. a: Bronze block formed in the casting experiment. The section marked by white lines was used for Sn isotope analyses. Fig. 2b: Molten metal was poured into a clay mold. Fig. 2c: Sampled parts of a slice of bronze block used for isotope analyses.

seven isotopes (114, 116, 117, 118, 120, 122, and 124) for Sn and two isotopes (121, 123) for Sb. Mass number 119 was monitored in place of 118 during analyses of Sn bead samples and bronze samples produced in the casting experiment to detect a possible mass-independent fractionation. A single isotope run consisted of 100 measurements of 5 s integration in each acquisition. All sample solutions were diluted to Sn = 60–100 ppb with 0.4 M HNO_3 containing trace amounts of HF. For 60 ppb solutions, we obtained total Sn signals of approximately 14×10^{-11} A. We also added a standard solution of Sb for mass bias correction (Clayton et al., 2002) such that the Sb concentration was 30–50 ppb.

Table 2
Procedure for separation of Sn (modified from Yamazaki et al. (2013)).

Operation	Solvents	
Washing	5 mL of 0.5 M HCl, 5 mL of Milli-Q	2 cycles
Conditioning	4 mL of 0.5 M HCl	
Loading	2 mL of 0.5 M HCl	
Cleaning 1	3 mL of 0.5 M HCl	
Cleaning 2	20 mL of 0.25 M HCl	
Sn collection	16 mL of 0.4 M HNO_3[a]	
Add	0.285 mL of 0.1 M HF	

[a] Sn containing fraction was evaporated to dryness for the samples of cast bronze (see text).

Mass fractionation correction during isotope analysis was conducted using a combination of external correction method and standard bracketing method, as described by Yamazaki et al. (2013). In this study, we applied the exponential law (Russell et al., 1978) using the following equation.

$$r_i = R_i \left(\frac{M_j}{M_k}\right)^{\beta} \quad (1)$$

Therein, r_i and R_i respectively represent the fractionation-corrected isotopic ratio and observed isotopic ratio for the element of interest. Also, M_j and M_k respectively stand for the masses of the target isotopes and the reference isotope. The mass bias factor, β, can be estimated from the following equation.

$$\beta = \frac{\ln\left(r_l^{ext} / R_l^{ext}\right)}{\ln\left(M_m^{ext} / M_n^{ext}\right)} \quad (2)$$

In that equation, r_l^{ext} and R_l^{ext} respectively represent the true and observed isotopic ratios for the doped element. Also, M_m^{ext} and M_n^{ext} respectively denote the masses of externally doped element (Sb). Following Longerich et al. (1987), we assumed the external standardization method in which the mass fractionation factor is assumed to be equal between the target element and doped element (herein, Sn and Sb, respectively). Although no Sb reference material has certified isotopic composition, we accepted $^{123}Sb/^{121}Sb = 0.7479$ (De Laeter et al., 2003) as the true isotopic ratio.

We also used the standard-sample bracketing method, in which a standard solution was measured before and after sample measurement. For this study, the corrected isotope ratios of a sample are expressed in δ notation as deviations from those of the SPEX standard solution calculated using the following equation.

$$\delta_{i_{SPEX}} = \frac{r_i^{sample} - r_i^{SPEX}}{r_i^{SPEX}} \times 10^3 \quad (3)$$

Therein, r_i^{SPEx} is the mean isotope ratio of SPEX measured before and after the target sample. This report describes the isotope composition of Sn with $\delta^{124}Sn/^{120}Sn$. Individual samples were analyzed separately three times. The average and 2SD of three measurements is reported.

We analyzed the Sn standard solution (NIST SRM 3161a) repeatedly to evaluate the long-term (about two months) reproducibility of isotope measurements. The Sn concentration in the

standard solution was fixed at 60 ppb. Then Sb was mixed to be 30 ppb for use in external standardization. The within-run precision for $^{124}Sn/^{120}Sn$ was better than 0.04‰ (2SE). The overall reproducibility of SRM 3161a measurements over two months was −0.30 ± 0.06‰ (Yamazaki et al., 2013).

Major element compositions of archaeological bronze samples were determined using an electron microscope (820; JEOL) with an energy dispersive X-ray analyzer (PV9550; Philips) at the National Museum of Japanese History. Quantitative analysis of the samples was performed using a focused beam of 15 kV accelerating voltage and 12 nA beam current. Standard materials of BNRM's (Brammer Non Destructive Reference Materials) Copper Based Alloys from Brammer Standard Company, INC. (Houston, USA) were used for the analyses.

Major element compositions of cast bronze were determined using an electron microprobe (JXA8800R; JEOL) at the Earthquake Research Institute, The University of Tokyo. Quantitative analysis of the cast bronze was performed using 15 kV accelerating voltage, 12 nA beam current, and a beam with 1 μm diameter.

Tin abundances in a cast bronze were determined using isotope dilution analysis after purification of Sn using IsoProbe, while copper abundances were determined using sensitivity method with an ICP mass spectrometer with a quadrupole mass analyzer (X-series II; Thermo Fisher) at the Earthquake Research Institute, The University of Tokyo. The uncertainties of Sn and Cu concentration were 0.1 and 0.5%, respectively.

4. Results and discussion

4.1. Casting experiment

The $\delta^{124}Sn/^{120}Sn$ values of five Sn beads used for the casting experiment were analyzed to examine the isotope compositions of raw materials. Results are shown in Table 3. No purification was conducted for the five bead samples. Results of bead analyses indicate that Sn beads have rather uniform isotope composition.

Table 3
Tin isotope ratios of Sn beads (raw material of cast bronze).

	Run	$\delta^{124}/^{120}Sn_{SPEx1}$ [‰]	2SE	2SD
Bead1	1	−0.15	0.04	
	2	−0.12	0.04	
	3	−0.11	0.03	
	average	−0.13		0.04
Bead2	1	−0.10	0.03	
	2	−0.02	0.03	
	3	−0.13	0.03	
	average	−0.08		0.12
Bead3	1	−0.10	0.03	
	2	−0.17	0.04	
	3	−0.12	0.03	
	average	−0.13		0.07
Bead4	1	−0.10	0.03	
	2	−0.10	0.04	
	3	−0.09	0.03	
	average	−0.10		0.01
Bead5	1	−0.16	0.03	
	2	−0.09	0.03	
	3	−0.06	0.03	
	average	−0.10		0.10
Average		−0.11		0.04

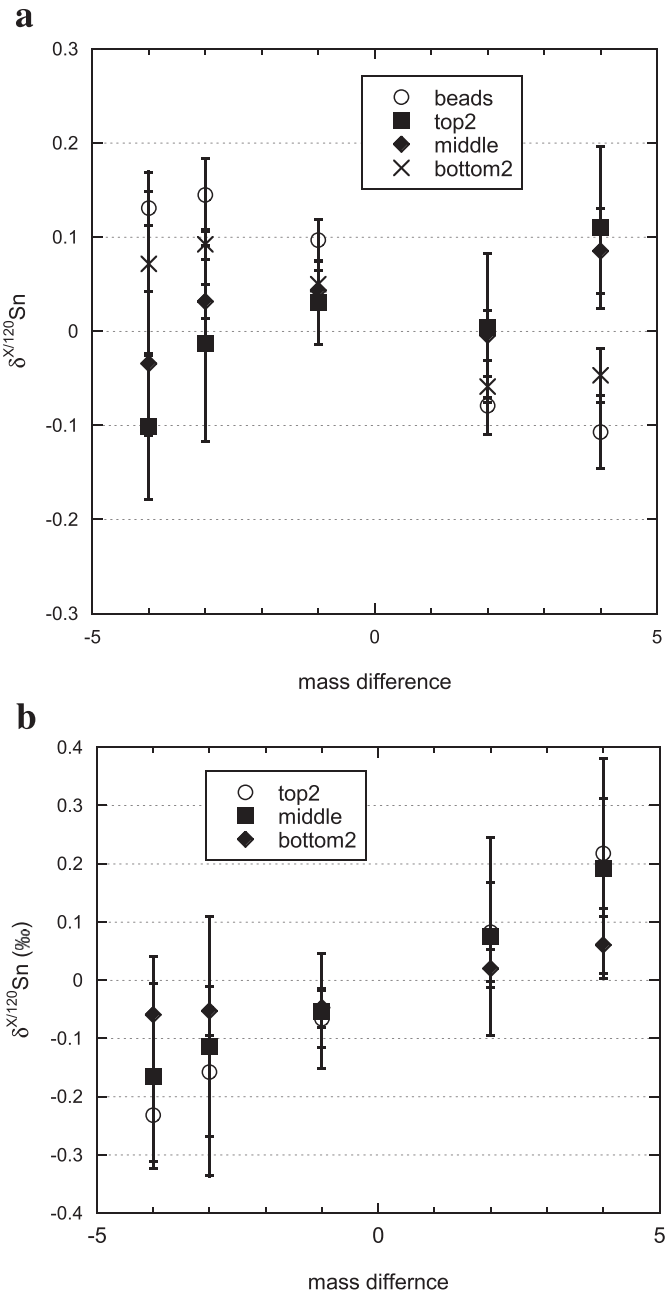

Fig. 3. a: δ-values of each mass pairs of the average of Sn beads (raw material of cast bronze) and cast bronze. Each sample solution was analyzed three times. Results are presented as averages. Error bars shown are 2SD. The influence of isotope fractionation during purification was corrected for bronze samples. Fig. 3b: Isotope fractionation between Sn beads and bronze samples. The δ-values of respective mass pairs are shown.

Five beads show $\delta^{124}Sn/^{120}Sn$ of −0.11 ± 0.04‰ (Table 3). Fig. 3a shows $\delta^{x}Sn/^{120}Sn$ vs. mass difference for the average of Sn beads. The plot shows that isotopes with odd mass numbers behaved differently from those with an even mass number. The mass-independent fractionation in odd isotopes of Sn was reported in some experiments such as liquid–liquid extraction, synthesis and UV irradiation (Malinovskiy et al., 2009; Moynier et al., 2009). Although the method for producing the Sn beads is unclear, it is likely that some processes to produce highly purified Sn beads caused the mass-independent fractionation. We use the average value of the five analyses as a starting isotope composition of raw

Table 4
Chemical compositions and Tin isotope ratios of cast bronze and fractionation during purification of mix standard solution.

	Run	$\delta^{124}/^{120}Sn_{SPEx1}$ [‰]	2SE	2SD	Corrected value [‰]	2SD	Cu (wt. %)	Sn (wt. %)
Top1	1	−0.05	0.04					
	2	0.02	0.03					
	3	0.02	0.03					
	Average	0.00		0.08	0.09	0.12		
Top2	1	0.08	0.03					
	2	0.00	0.03					
	3	0.01	0.03					
	Average	0.03		0.09	0.13	0.12	85	15.1
Average		0.02		0.06	0.11	0.10		
Middle	1	−0.02	0.04					
	2	0.02	0.03					
	3	−0.03	0.03					
	Average	−0.01		0.04	0.09	0.09	85	15.0
Bottom1	1	−0.12	0.04					
	2	−0.13	0.03					
	3	−0.11	0.03					
	Average	−0.12		0.02	−0.03	0.09		
Bottom2	1	−0.15	0.04					
	2	−0.15	0.03					
	3	−0.13	0.04					
	Average	−0.14		0.03	−0.05	0.09	87	13.1
Average		−0.13		0.02	−0.04	0.08		
Mix standard (Cu–Sn–Pb)	Run	$\delta^{124}/^{120}Sn_{SPEx1}$ [‰]	2SE	2SD				
	1	−0.08	0.04					
	2	−0.07	0.04					
	3	−0.14	0.04					
	Average	−0.10		0.08				

Sampling positions are shown in Fig. 2c. The value of the mix standard solution was used for the correction of isotope fractionation during purification for the cast bronze.

material of Sn in the following discussions related to the casting experiment.

Table 4 presents results of Sn isotope analyses and chemical composition analyses on a bronze block produced in the casting experiment. The Sn isotope composition of two samples from the top and bottom parts and one sample from the medium part were analyzed (Fig. 2c), whereas chemical compositions of the top 2, middle 2, and bottom 2 were analyzed. Tin was purified from bronze solutions and the isotope ratios reported for the samples of a bronze block were corrected for isotope fractionation during purification as shown in Table 4. Table 4 shows that Sn concentrations of the top 2, middle 2, and bottom 2 were, respectively, 15.1, 15.0 and 13.1 weight%, while Cu concentrations were 85, 85, and 87 weight%. Fig. 4 presents the distribution of Sn isotope composition in the bronze block. The $\delta^{124}Sn/^{120}Sn$ values of two samples from the block surface part were 0.09 ± 0.12 and 0.13 ± 0.12‰, whereas those of two bottom parts were −0.03 ± 0.09 and −0.05 ± 0.09‰. One analysis of the middle part showed $\delta^{124}Sn/^{120}Sn$ of 0.09 ± 0.09‰. The results suggest that the surface part of the block was slightly enriched in heavy Sn isotopes compared with the bottom part, although isotope ratios of the two parts overlapped when the uncertainty introduced into the purification process is considered. Fig. 3b shows mass fractionations between parts of the cast bronze and Sn beads. All parts show linear correlation, suggesting that mass-dependent fractionation occurred in the casting process.

The differences in chemical and isotope compositions in the bronze block can be interpreted as follows. When molten metal was poured into the clay mold, which was left overnight at room temperature, molten metal started solidification from the edges touching the clay mold. The phase diagram of bronze indicates that the first solid of mixture of Cu and Sn is enriched in Cu, whereas the residual liquid becomes enriched in Sn. Consequently, the bottom samples, enriched in Cu, solidified at an early stage, while the top and middle samples solidified later. The heterogeneity observed inside of the bronze block, 0.15‰, in the averages of top and bottom samples, was greater than the isotope heterogeneity of Sn beads.

The observed isotope heterogeneity might be the result of two processes: (1) isotope fractionation between solidified and molten metal and (2) isotope fractionation caused by evaporation. It is difficult to decide which process caused the heterogeneity, but it is likely that evaporation is more important for the following reasons. Bigeleisen and Mayer (1947) showed that heavy isotopes tend to concentrate in stronger bonding. It is anticipated that fractionation between the solid and liquid phases concentrates heavier isotopes

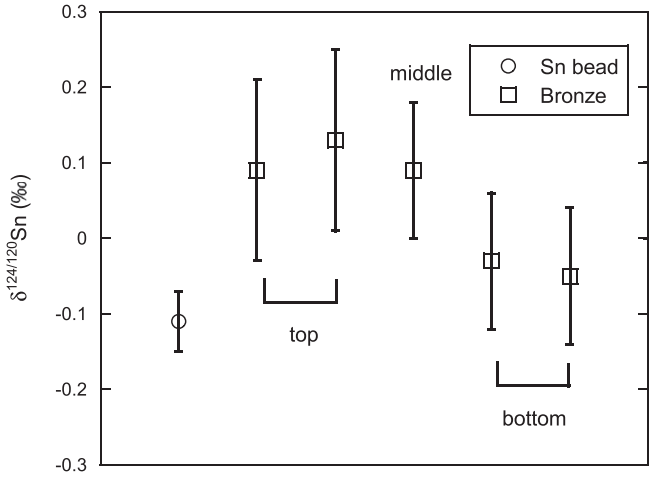

Fig. 4. Spatial variation in Sn isotope composition in the bronze block. Isotope variation between Sn bead (material) and casted bronze is shown. The circle symbol represents a Sn bead. Squares are the parts of casted bronze. Bronze data were corrected for isotope fractionation during purification.

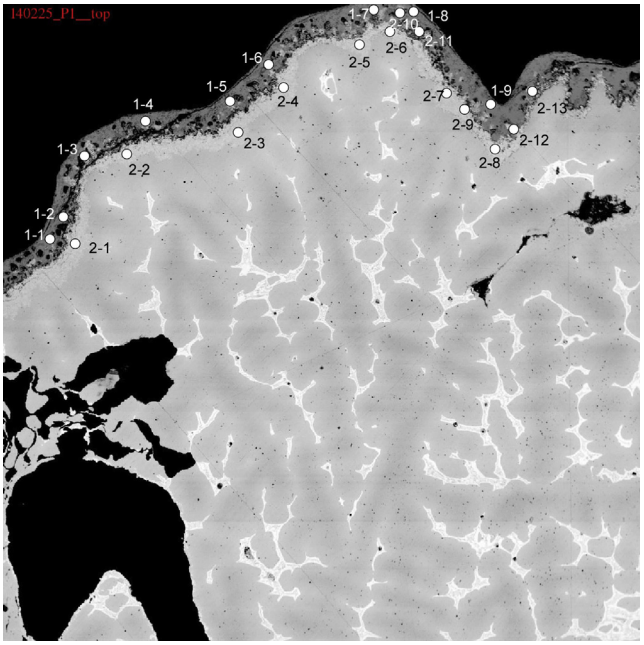

Fig. 5. Composite image of the surface part of the cast bronze with positions of electron microprobe analyses. Their chemical compositions are shown in Table 5.

in the solid phase, as shown in the case of an ice-water system (Lehmann and Siegenthaler, 1991). Therefore, when the bottom part of the bronze melt first solidified, we inferred that the bottom part would be enriched in heavy isotopes, which is not consistent with the observed results.

Kazenas et al. (1996) and Zimmermann et al. (1996) analyzed evaporation of Sn compounds using high-temperature mass spectrometry. They reported that $Sn_nO_n^+$ species ($n = 4, 2, 1, 6$) were the main components of vapor over the $Sn_{(l)} + SnO_{2(s)}$ melt mixture at temperatures of 600–1150 °C. Evaporation of oxidized Sn was also supported by electron microprobe observations of the cast bronze. Fig. 5 shows a composite image of the surface part of the bronze block. The eutectoid structure is ubiquitous in the block. Oxidized zones are distributed along the surface and in openings inside of the block. Table 5 presents results of electron microprobe analyses. Some points in the oxidized zone contain little Sn, suggesting evaporation loss. Consequently, it is likely that a part of molten Sn was oxidized to SnO_2 in the clay mold and compounds of Sn_nO_n evaporated from residual molten metal and that the bottom part was solidified before evaporation of Sn_nO_n started.

By comparing the isotope composition of the bottom part of the bronze block, which was solidified soon after molten metal was poured into the pod, with that of the Sn beads, it is possible to evaluate the extent of isotope fractionation that occurred while Sn and Cu metals were melted in the graphite pod. The $\delta^{124}Sn/^{120}Sn$ of two samples of bottom parts were -0.03 ± 0.09 and -0.05 ± 0.09‰, which are consistent with the average of Sn beads ($\delta^{124}Sn/^{120}Sn = -0.09 \pm 0.11$‰). The consistency suggests that no significant isotope fractionation occurred when Cu and Sn metals were heated in the graphite pod. The isotope difference between Sn beads and the bottom part of the bronze block was smaller than that between the average values of the upper part and the bottom part of the bronze block. We were able to expect larger isotope fractionation by evaporation during molten metal heating in the graphite pod because the molten metal was kept at 1100–1200 °C for longer time. The absence of fractionation suggests that Sn was not oxidized under the reducing environment in the graphite pod

Table 5
Chemical compositions of cast bronze.

Point	Cu (%)	Sn (%)	O (%)
Surface1-1	68.0	0.0	32.0
Surface1-2	70.7	0.0	29.3
Surface1-3	67.1	0.0	32.9
Surface1-4	66.6	0.0	33.4
Surface1-5	65.1	0.0	34.9
Surface1-6	67.8	0.0	32.2
Surface1-7	66.8	0.0	33.2
Surface1-8	67.5	0.0	32.5
Surface1-9	59.3	3.5	37.2
Surface2-1	32.0	18.3	49.6
Surface2-2	62.6	11.9	25.6
Surface2-3	9.4	24.2	66.4
Surface2-4	20.6	24.6	54.8
Surface2-5	65.6	13.9	20.5
Surface2-6	42.2	18.3	39.5
Surface2-7	52.0	17.5	30.5
Surface2-8	78.8	11.0	10.2
Surface2-9	59.4	13.0	27.5
Surface2-10	37.3	18.6	44.1
Surface2-11	12.2	21.3	66.5
Surface2-12	8.5	23.2	68.3
Surface2-13	40.1	12.5	47.5

Chemical compositions were analyzed at ERI, The University of Tokyo (see Section 3).

Table 6
Sn isotope compositions of bronzes.

Sample	Run	$\delta^{124}/^{120}Sn_{SPEx1}$ [‰]	2SE	2SD
1807	1	−0.77	0.03	
	2	−0.78	0.03	
	3	−0.71	0.03	
	Average	−0.75		0.08
	Corrected*	−0.09		0.12
1813	1	−0.84	0.03	
	2	−0.78	0.03	
	3	−0.83	0.03	
	Average	−0.82		0.06
	Corrected	−0.15		0.10
1827-3	1	−0.58	0.03	
	2	−0.66	0.03	
	3	−0.62	0.04	
	Average	−0.62		0.08
	Corrected	0.05		0.11
1829	1	−0.78	0.03	
	2	−0.77	0.03	
	3	−0.78	0.03	
	Average	−0.78		0.02
	Corrected	−0.11		0.09
1950	1	−1.04	0.03	
	2	−1.02	0.03	
	3	−1.02	0.03	
	Average	−1.03		0.03
	Corrected	−0.36		0.09
1953	1	−0.69	0.03	
	2	−0.66	0.03	
	3	−0.66	0.03	
	Average	−0.67		0.03
	Corrected	0.00		0.09
Average	Recalc	−0.11		0.29

Correction of isotope fractionation during purification was made using the value, -0.66 ± 0.09‰ in $\delta^{124}Sn/^{120}Sn$ scale, reported in Yamazaki et al. (2013).

and that little SnO was evaporated. Gale et al. (1999) investigated smelting and refining processes' ability to cause isotope fractionation by comparing copper isotope compositions of malachite ore, copper metal, and slag. They observed no marked isotope fractionation for Cu among the three samples. Consequently, they concluded that smelting causes no marked isotope shift in Cu. The results of our casting experiment also suggest that smelting process under reducing condition would not cause a significant isotope shift in Sn, although the evaporation mechanism is apparently different between the two elements. If used bronze was melted under oxidizing condition for recycled use, however, isotope shift of bronze might occur. Further experimentation is necessary to elucidate this phenomenon.

4.2. Excavated bronze products from China

We analyzed six bronze samples excavated from China. Details of Sn isotope compositions for these samples are presented in Table 6. All samples of bronze products analyzed in this study showed mass-dependent fractionation (two examples are shown in Fig. 6). No mass-independent fractionation was found. The $\delta^{124}Sn/^{120}Sn$ values of six bronze samples present rather limited variation of −0.36 to 0.05‰ as shown in Fig. 7a (1807, 1813, 1827-3, 1829, 1950 and 1953 are, respectively, −0.09 ± 0.12, −0.15 ± 0.10, 0.05 ± 0.11, −0.11 ± 0.09, −0.36 ± 0.09, and 0.00 ± 0.09‰). Balliana et al. (2013) reported $\delta^{122}Sn/^{116}Sn$ values of 11 bronze samples, of which the variation was nearly 1.0‰. The variation of the Sn isotope ratio in our six bronze samples (0.41‰) was less than half of that reported by Balliana et al. (2013). It becomes much smaller (0.2‰) when sample 1950 is excluded. Fig. 7b shows $\delta^{124}Sn/^{120}Sn$ values of bronzes compared to those of cassiterites from Asian countries including China. Although available isotope data of cassiterites are limited, we will compare the Sn isotope compositions of bronze and cassiterites. Haustein et al. (2010) reported significant isotopic variations in cassiterites from two ore deposits. Yamazaki et al. (2013) analyzed one cassiterite from most of ore deposits except

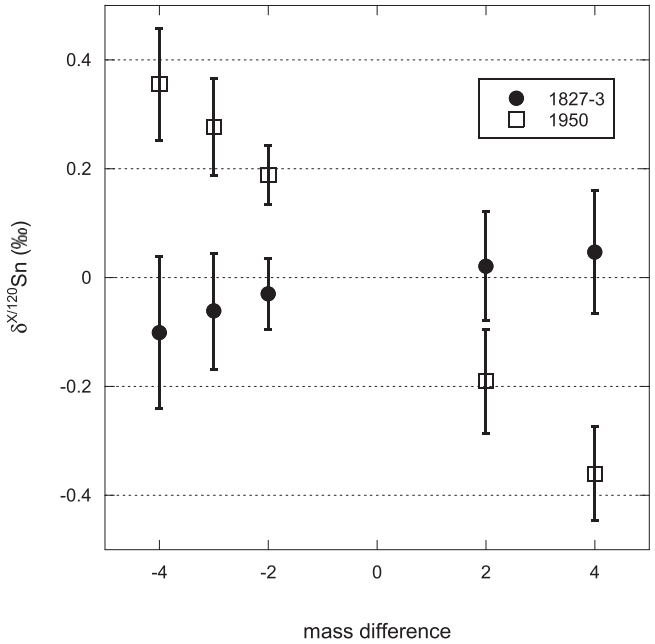

Fig. 6. δ-values of each mass pair of two bronzes (1827-3 and 1950) excavated from China. We analyzed each sample solution three times. Results are presented as averages. Error bars shown are 2SD. The influence of isotope fractionation during purification was corrected. Both samples show mass-dependent isotope fractionation.

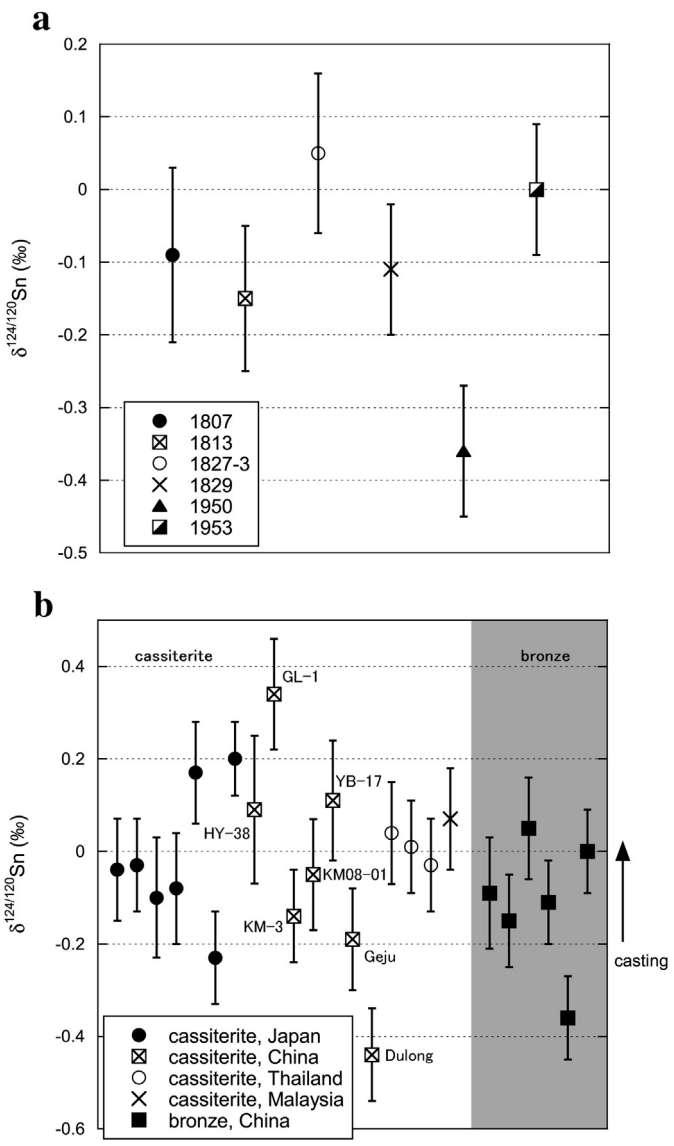

Fig. 7. a: Tin isotope ratios of bronze specimens excavated from China. Isotope measurements were repeated three times for each sample. The uncertainties shown are 2SD of the three measurements. Fig. 7b: Delta values of cassiterite (data from Yamazaki et al., 2013) and bronze samples. Symbols in the clear area represent cassiterite. Sample names are shown for Chinese cassiterites. Symbols in the shaded area represent bronze artifacts. Right side arrow shows the direction and magnitude of the fractionation observed in our casting experiment.

two. Two cassiterites from the Kamst deposit in China and two cassiterites from the Kosaba mine in Thailand showed identical isotope compositions within the uncertainties. Although Sn isotope homogeneity in a single ore deposit is to be confirmed in future study, we will use available data base in the following discussions.

In the following discussions, we will use the observation in the casting experiment that bronze experienced casting tends to have heavier Sn isotope composition.

The δ-values of bronze artifacts were generally consistent with those of cassiterite samples, HY38 (Sareshike, Xinjiang), KM3 (Kamst, Xinjiang), KM08-1 (Kamst, Xinjiang), YB-17 (Yanbei, Jiangxi), Gejiu (Geju, Yunnan), and Dulong (Dulong, Yunnan), within analytical uncertainty. A significant difference was found between bronze artifacts and cassiterite of GL1 (Ganliangzi, Xinjiang). The tin isotopic composition of GL1 is heavier than that of bronze artifacts, so it is unlikely that Sn ore from Ganliangzi

deposits were used as a source material of bronze products excavated in Liulihe and Panlongcheng.

The value of $\delta^{124}Sn/^{124}Sn$ of sample 1950 resembles that of a cassiterite from the Dulong deposit, Yunnan. It is noteworthy that sample 1950 cannot be derived from other cassiterite samples analyzed in this study for the reason described above.

Penhallurick (1986) stated that the area of the Nanling Mountain Range was a major Sn resource. Most Nanling Mountain Range deposits are concentrated in Yunnan Province. Gejiu district is a representative area where main ore veins exist in granites associating with limestone (Jones, 1925). Tin also yields from Jiangxi Province (such as Ta-yu and Nan-k'ang) and Hunan Province (Ch'ang-ning and Lin-wu) in the tin belt of Nanling. Some dispute has arisen as to whether northern China, where Panlongchen and Liulihe are located, had links with the southern regions including Nanling Mountain Range during the Shang and Zhou dynasties. Jin (1987) analyzed Pb isotope ratios for bronze samples unearthed from Fu-hao's tomb at Yinxu in Anyang, which was dated as the later period of the Shang Dynasty. He discovered that Pb isotope ratios of those bronze samples were in agreement with that of ores from the eastern part of Yunnan Province and suggested that the bronzes of the late Shang dynasty had been manufactured using Pb ores from Yunnan Province in southern China. On the other hand, Penhallurick (1986) reported the possibility that the Shang Dynasty used tin sources distributed near Anyang. Several Sn deposits in northern China were reported by Wang et al. (2005), Niu et al. (2008), and Zhai et al. (2012). Among these studies, Wang et al. (2005) stated that the southern part of the Da Hinggan Mountains is the most important Sn polymetallic concentration region in northern China. Consequently, cassiterites from northern China should be analyzed to clarify their provenance. Apart from northern China, the possibility exists that cassiterite from the Yanbei deposit in Jiangxi province (YB-17) was a raw material of bronze artifacts. The sample of YB-17, 0.11 ± 0.13‰, has a similar Sn isotope ratio to those of the bronze artifacts analyzed in this study. The ore is located nearest the cities of the Shang dynasties. However, we can deny the possibility that the Yanbei deposit was used as a Sn source for the two bronze artifacts in Shang dynasty (1813 and 1829) and a bronze artifact (1953) in Zhou dynasty for the reason presented above.

The samples from Liulihe (1950, 1953), Zhou Dynasty, have significantly different isotope ratios. Sample 1950 is enriched in lighter isotopes. Considering that sample 1950 is enriched in lighter isotopes, its unique isotope composition is difficult to ascribe to casting. It is more likely to be ascribed to a difference in raw materials (Sn ores). It is unlikely that sample 1950 was produced by Sn ores from Yanbei deposit. However, its Sn isotope composition agrees with that of a cassiterite from Dulong. We can present the possibility that the Sn origin of sample 1950 excavated from Liulihe was southern China for the reasons described above. Sun et al. (2001) analyzed Pb isotope ratios of bronze products including samples analyzed in this study. They reported that Pb isotope compositions had large variations and concluded that more than two sources of Pb should have been present. The Sn isotope compositions show rather limited variation, which could have been generated after several castings. However, our results indicate the possible use of Sn isotope composition for provenance studies, as described above. It has been disputed whether Sn was supplied from deposits in northern China or imported from the Yunnan to Shang Dynasty. Further work is expected to shed light on this question.

5. Concluding remarks

The casting experiment results revealed that slight but detectable isotope fractionation was introduced during casting by the preferential evaporation of light isotopes of Sn. It was likely that slight heterogeneity in Sn isotope composition was also introduced into a bronze object. However, the influence of evaporation was limited. It is likely that most of the bronze product retains the original Sn isotope composition if metal source materials were melted in a reducing condition.

Sn isotope analyses of Chinese bronze products revealed small but detectable variation in $\delta^{124}Sn/^{120}Sn$ as large as 0.4‰ in bronze artifacts. The variation surpassed the extent of isotope fractionation shown by the casting experiment. Because the variation of Sn isotope ratio in cassiterites and bronze products is limited, Sn isotope tracer is not always useful to discriminate an origin of Sn used for a bronze. Our preliminary results, however, suggest the potential benefits of Sn isotope composition to put constraint on the provenance of a bronze with a distinct isotope property.

Acknowledgments

This research was supported by a Grant-in-Aid for Scientific Research of the Ministry of Education, Culture, Sports, Science and Technology (MEXT), Japan, #23300322, to SN. EY is supported by Global COE program, From the Earth to "Earths". We also appreciated Ms. S. Shibata for her help in casting experiments. Discussions with Dr. T. Nagae are also acknowledged. Comments from three anonymous reviewers improved the manuscript.

References

Balliana, E., Aramendía, M., Resano, M., Barbante, C., Vanhaecke, F., 2013. Copper and tin isotopic analysis of ancient bronzes for archaeological investigation: development and validation of a suitable analytical methodology. Anal. Bioanal. Chem. 405, 2973–2986.
Bigeleisen, J., Mayer, M.G., 1947. Calculation of equilibrium constants for isotopic exchange reactions. J. Chem. Phys. 15, 261–267.
Budd, P., Haggerty, R., Pollard, A.M., Scaife, B., Thomas, R.G., 1995. New heavy isotope studies in archaeology. Isr. J. Chem. 35, 125–130.
Clayton, R., Andersson, P., Gale, N.H., Gillis, C., Whitehouse, M., 2002. Precise determination of the isotopic composition of Sn using MC–ICP–MS. J. Anal. At. Spectrom. 17, 1248–1256.
De Laeter, J.R., Jeffery, P.M., 1965. The isotopic composition of terrestrial and meteoritic tin. J. Geophys. Res. 70, 2895–2903.
De Laeter, J.R., Jeffery, P.M., 1967. Tin: its isotopic and elemental abundance. Geochim. Cosmochim. Acta 31, 969–985.
De Laeter, J.R., Böhlke, J.K., De Biévre, P., Hidaka, H., Peiser, H.S., Rosman, K.J.R., Taylor, P.D.P., 2003. Atomic weights of the elements: review 2000. Pure Appl. Chem. 75, 683–800.
Devillers, C., Lecomte, T., Hagemann, R., 1983. Absolute isotope abundances of tin. Int. J. Mass Spectrom. Ion Phys. 50, 205–217.
Gale, N.H., 1997. The isotopic composition of tin in some ancient metals and the recycling problem in metal provenancing. Archeometry 39, 71–82.
Gale, N.H., Woodhead, A.P., Stos-Gale, Z.A., Walder, A., Bowen, I., 1999. Natural variations detected in the isotopic composition of copper: possible applications to archaeology and geochemistry. Int. J. Mass Spectrom. 184, 1–9.
Haustein, M., Gillis, C., Pernicka, E., 2010. Tin isotopy – a new method for solving old questions. Archaeometry 52, 816–832.
Hubei Provincial Institute of Cultural Relics and Archaeology, 2001. Panlongcheng: 1963–1994 Archaeological Excavation Report. Cultural Relics Press.
Jin, Z.Y., 1987. A study of the mineral resources of tin contained in the Central Plains Bronze of later period of the Shang Dynasty. J. Dialectics Nat. 9, 47–55 and 80 (in Chinese with English abstract).
Jones, W.R., 1925. Tinfields of the World. Mining Publications.
Kazenas, E., Bol'shikh, M., Petrov, A., 1996. Thermodynamics of processes of vaporization, dissociation, and gad-phase reactions in vapors over tin–oxygen system. Russ. Metall. 3, 23–29.
Lee, D.C., Halliday, A.N., 1995. Precise determinations of the isotopic compositions and atomic weights of molybdenum, tellurium, tin and tungsten using ICP magnetic sector multiple collector mass spectrometry. Int. J. Mass Spectrom. Ion Process. 146/147, 35–46.
Lehmann, M., Siegenthaler, U., 1991. Equilibrium oxygen- and hydrogen-isotope fractionation between ice and water. J. Glaciol. 37, 23–26.
Liulihe Archaeology Team, 1990. The Brief Excavation Report of No. 1193 Tomb Liulihe Site. Archaeology, Beijing, pp. 20–31.
Longerich, H.P., Freyer, B.J., Strong, D.F., 1987. Determination of lead isotope ratios by inductively coupled plasma-mass spectrometry (ICP-MS). Spectrochim. Acta B At. Spectrosc 42, 39–48.

Loss, R.D., Rosman, K.J.R., De Laeter, J.R., 1990. The isotopic composition of zinc, palladium, silver, cadmium, tin, and tellurium in acid-etched residues of the Allende meteorite. Geochim. Cosmochim. Acta 54, 3525–3536.
Malinovskiy, D., Moens, L., Vanhaecke, F., 2009. Isotopic fractionation of Sn during methylation and demethylation. Environ. Sci. Technol. 43, 4399–4404.
McNaughton, N.J., Loss, R.D., 1990. Stable isotope variations of tin. In: Herbert, H.K., Ho, S.E. (Eds.), Stable Isotopes and Fluid Processes in Mineralization. Geol. Dept. & Univ. Ext., Univ. W, Australia, pp. 269–276.
McNaughton, N.J., Rosman, K.J.R., 1991. Tin isotope fractionation in terrestrial cassiterites. Geochim. Cosmochim. Acta 55, 499–504.
Moynier, F., Fujii, T., Télouk, P., 2009. Mass-independent isotopic fractionation of tin in chemical exchange reaction using a crown ether. Anal. Chim. Acta 632, 234–239.
Nickel, D., Haustein, M., Lampke, T., Pernicka, E., 2012. Identification of forgeries by measuring tin isotopes in corroded bronze objects. Archaeometry 54, 167–174.
Niu, S.Y., Sun, A.Q., Wang, B.D., Liu, J.M., Guo, L.J., Hu, H.B., Xu, C.S., 2008. Sources of ore-forming materials and mineralization of the Dajing Cu-Sn polymetallic deposit, Inn Mong. Geol. China 35, 714–724 (in Chinese with English abstract).
Osawa, T., Ono, M., Esaka, F., Okayasu, S., Iguchi, Y., Hao, T., Magara, M., Mashimo, T., 2009. Mass-dependent isotopic fractionation of a solid tin under a strong gravitational field. Eur. Phys. Lett. 85, 64001.
Penhallurick, R.D., 1986. Tin in Antiquity: its Mining and Trade Throughout the Ancient World with Particular Reference to Cornwall. Institute of Metals, London.
Rapp, G., 2009. Archaeo-mineralogy, second ed. Springer-Verlag, Berlin Heidelberg.
Radivojević, M., Rehren, T., Kuzmanović-Cvetković, J., Jovanović, M., Northover, J.P., 2013. Tainted ores and the rise of tin bronzes in Eurasia, *c.* 6500 years ago. Antiquity 87, 1030–1045.
Rosman, K.J.R., McNaughton, N.J., 1987. High-precision measurement of isotopic fractionation in tin. Int. J. Mass Spectrom. Ion Process. 75, 91–98.
Rosman, K.J.R., Loss, R.D., De Laeter, J.R., 1984. The isotopic composition of tin. Int. J. Mass Spectrom. Ion Process. 56, 281–291.
Russell, W.A., Papanastassiou, D.A., Tombrello, T.A., 1978. Ca isotope fractionation on the Earth and other solar system materials. Geochim. Cosmochim. Acta 42, 1075–1090.
Stos-Gale, Z.A., Gale, N.H., 2009. Metal provenancing using isotopes and the Oxford archaeological lead isotope database (OXALID). Archaeol. Anthropol. Sci. 1, 195–213.
Sun, S., Han, R., Chen, T., Saito, T., Sakamoto, M., Taguchi, I., 2001. The report of lead isotope ratios of bronze objects excavated from the Panlongcheng Site (in Chinese). In: The Panlongcheng Site Report of Archaeological Excavation from 1963–1994. The Hubei Provincial Institute of Cultural Relics and Archaeology, 2001, vol. 1(I). Cultural Relics Publishing House, pp. 545–551.
Wang, J.B., Wang, Y.W., Wang, L.J., 2005. Tin-polymetallic metallogenic series in the southern part of Da Hinggan Mountains, China. Geol. Prospect. 41, 15–20 (in Chinese with English abstract).
Yamazaki, E., Nakai, S., Yokoyama, T., Ishihara, S., Tang, H., 2013. Tin isotope analysis of cassiterites from Southeastern and Eastern Asia. Geochem. J. 47, 21–35.
Yi, E., Halliday, A.N., Lee, D.-C., Christensen, J.N., 1995. Indium and tin in basalts, sulfides, and the mantle. Geochim. Cosmochim. Acta 59, 5081–5090.
Zhai, D.-G., Liu, J.-J., Yang, Y.-Q., Wang, J.-P., Ding, L., Liu, X.-W., Zhang, M., Yao, M.-J., Su, L., Zhang, H.-Y., 2012. Petrogenetic and metallogenic ages and tectonic setting of the Huangganglang Fe-Sn deposit, Inner Mongolia. Acta Petrol. Mineral. 31, 513–523 (in Chinese with English abstract).
Zimmermann, E., Konigs, S., Neuschutz, D., 1996. Determination by mass spectrometry of the partial pressures of SnO, Sn_2O_2, Sn_4O_4 and Sn_6O_6 in equilibrium with oxygen saturated tin melts. Z. Fur Phys. Chem. 193, 195–206.